ELSEVIER

Three dimensional surface topography characterization of the electron beam melted Ti6Al4V

SPECIAL FEATURE

Alfred T. Sidambe

Bioengineering & Health Technologies Group, School of Clinical Dentistry, University of Sheffield, 19 Claremont Crescent, SHEFFIELD, S10 2TA UK

The properties of the components fabricated via electron beam melting (EBM) are known to be affected by different processing parameters such as beam current, offset focus, scan speed, layer thickness, powder size and part orientation. This clearly has part design, placement and performance implications and therefore in this study, the effect of part orientation on the surface topography of the EBM Ti6Al4V alloy was investigated. Three different surface finishes were obtained by fabricating disc components in the horizontal (0°), inclined (55°) and vertical (90°) in the EBM build chamber. Their resulting amplitude surface topographies were characterized through white light interferometry and scanning electron microscopy. Comparison of the results revealed a significant difference in numerical values of the 3-D surface roughness parameters. For the average roughness, the horizontal (0°) surface had a smoother surface (S_a = 15.8 μm) whereas the inclined (55°) and vertical (90°) surfaces had rougher surface characteristics with and S_a = 36.8 μm and 54.3 μm respectively. The results showed that part orientation of titanium during EBM can produce surfaces with different characteristics due the anisotropic melting of the powders by the EBM process leading to part design considerations and complexities associated with EBM parts. The selection of the 3-D surface topography parameters and surface morphology characterization were also shown to address the inadequacies of two-dimensional (2-D) surface analysis.

Introduction

Titanium (Ti) and titanium alloys are an excellent choice for aerospace, medical, oil and gas, power generation, high-end automotive and sporting applications because they exhibit good biocompatibility, a high specific strength and excellent corrosion resistance [1–3]. However, the widespread use of titanium and its alloys has been limited by high cost due to the multi-step Kroll extraction process of the Ti raw material [4,5]. Titanium production is also hampered by the high cost in traditional manufacturing processes, and poor workability for complex shape production. This has led to numerous investigations of various potentially lower-cost processes which involve net-shape manufacturing [4]. Powder net-shape routes of titanium processing have emerged as techniques that can minimize the cost of production, particularly for complex shapes [6]. Various manufacturing routes which utilize powder metallurgy have been reviewed by Froes [7] and Sidambe [6]. Advanced additive manufacturing (AM) processes such as powder bed fusion offer design flexibility for fabricating products that have complicated shapes with a relatively very high accuracy and products also meet the demands of low-volume customized manufacturing [8]. Additive manufacturing comprises a cluster of technologies that have emerged in the last two decades. In AM the objects are created by adding the material one cross-sectional layer at a time and AM is therefore distinct from traditional machining techniques, which mostly rely on the removal of material by methods such as cutting or drilling (subtractive manufacturing) [9–11]. AM makes use of the additive method

E-mail address: a.t.sidambe@gmail.com.

 http://dx.doi.org/10.1016/j.mprp.2017.02.003

Please cite this article in press as: A.T. Sidambe, Met. Powder Rep. (2017), http://dx.doi.org/10.1016/j.mprp.2017.02.003

to form a three-dimensional (3-D) solid object of almost any shape from a computer aided drawing (CAD) model [6].

AM technologies include fused deposition modeling, laser micro-sintering, direct metal laser sintering (DMLS), three-dimensional (3-D) laser cladding, electron beam melting (EBM), and electron beam sintering (EBS) [12,9]. The DMLS and EBM processes are two of the additive manufacturing techniques mainly used for metals. In the EBM process the surface roughness and size of the minimum features is significantly higher than in other processes such as DMLS. In the EBM system the parts are manufactured by melting of the metal powder, layer by layer using a magnetically directed electron beam under a high vacuum atmosphere [13]. The presence of this high vacuum atmosphere in EBM is particularly suited for the manufacturing of titanium and titanium alloys [14]. Furthermore, the EBM process takes place at an elevated temperature (>800 °C) and the additional surface sintering can significantly affect the surface quality of the fabricated parts. More details about the process including a schematic drawing of an electron beam melting system have been published elsewhere [15–17].

Part of the challenges of using EBM in manufacturing is therefore to optimize the surface finish of the as-built components in order to meet part specification requirements [18,19]. It has been reported that surface texture significantly affects functionality of a component and that in some applications up to 10% of part failure rate for manufactured parts is due to surface effects [20]. When additive manufacturing is taken into account, the failure rate is expected to increase [8]. On the other hand AM has made significant breakthroughs in biomedical applications because the resultant surfaces can be tailored to influence osseointegration [6]. The influences of the surface topography and how it affects the final properties of biomedical devices has already attracted a number of studies [6,14,21–23]. Since the surface texture is affected on the EBM by processing parameters such as beam current, hatch distance, part orientation and powder particle size, it is therefore controllable during processing where post processing is either not desirable or it is to be avoided and where the part geometry cannot be changed [1,19,24]. There are further challenges in that inner cores may not be accessible for post-processing.

This study has been carried out because of the implications for the design and part placement that manufacturing Ti-64 via the EBM process brings. When fabricating parts in the EBM, the engineer has to consider a number of factors related to part orientation. The build height and build time can be reduced by the way the component is oriented. Furthermore there is an angle of orientation above which the need for supports is eradicated and at which residual stresses are reduced [25]. The ability to estimate the specific surface quality within an area of a part can be realized by studies such as this one which investigate the angle-dependent surface characteristics [8]. Thus, three different surface finishes were obtained by fabricating disc components in the horizontal (0°), inclined (55°) and vertical (90°) orientations with respect to the EBM build chamber. The 3-D statistical height distribution parameters were selected because they are expected to be more accurate than the widely used 2-D profile parameters which are a representation of the roughness profile along a plane section [26,27]. In AM, the layering phenomenon and hatch strategies are also known to contribute to the surface roughness of parts and it is essential to capture the surface roughness along the 3-D amplitude direction. A variation of the measurement position can correspond to a significant variation of the parameter values and therefore a reasonable analysis of aperiodic surface structures with only one single profile line is not recommended [28]. This study has also been carried out in order to demonstrate the degree to which selected parameters are effective at representing the geometry of the surfaces specific to the additive manufacturing process.

Materials and experimental techniques

Titanium discs

In order to carry out this study disc components (2 mm thick, 10 mm diameter each) were manufactured. The titanium alloy Ti-64 supplied by Arcam AB, with a nominal particle size range of 45 μm to 105 μm was melted in the Arcam S12 EBM system (Arcam AB, Molndal, Sweden). Standard melt themes encompassing the beam current, offset focus and scan speed for the Ti-64 powder were used along with a layer thickness of 70 μm and therefore were kept constant whilst the study focused on the effect of part orientation. Three different surface roughnesses were obtained by orienting the builds in horizontal (0°), inclined (55°) and vertical (90°) orientations in the EBM build chamber.

Figure 1 shows a CAD illustration of orientation of the Ti-64 discs within the build preparation software. The angles of orientation were calculated with reference to the horizontal axis (x-y Cartesian plain). After the parts were manufactured on the EBM machine, powder blasting was used to remove loose metallic particles from the surfaces of the parts.

Surface characteristics

The characterization of the surface topographies was carried out using the Contour GT 3-D Optical Profiler (Bruker UK Ltd, Coventry, UK). The profiler was used in conjunction with the Vision64™ software. The Contour GT is based on the fundamental science of white light interferometry and is designed to deliver high resolution images and surface measurements [27]. The optical system was also preferred to other systems such as atomic force microscopes

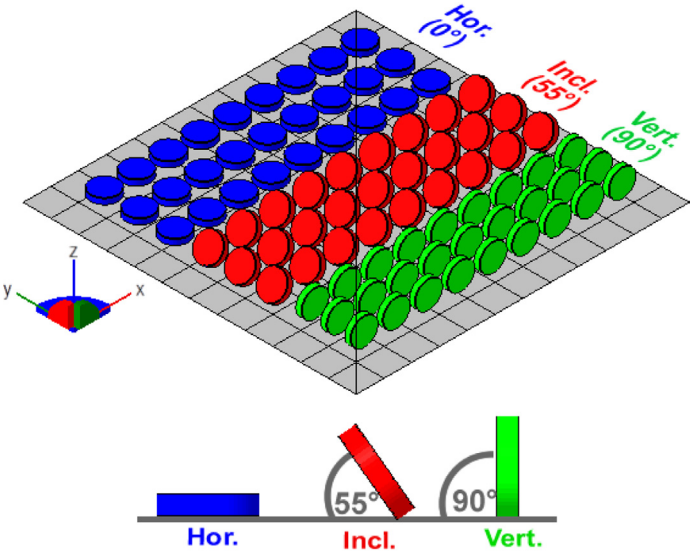

FIGURE 1
CAD illustration of the part orientations of the Ti-64 discs within the build preparation software.

Please cite this article in press as: A.T. Sidambe, Met. Powder Rep. (2017), http://dx.doi.org/10.1016/j.mprp.2017.02.003

TABLE 1

Surface characteristics of the EBM discs characterized through interferometry.

Surface	S_a (μm)	S_q (μm)	S_{ku} (μm)	S_{sk} (μm)	S_p (μm)	S_v (μm)	S_z (μm)
Horizontal (0°)	15.8	18.9	2.4	−0.162	48.5	−58.9	107.4
Inclined (55°)	36.8	49.9	6.1	1.2	330.3	−579.1	909.5
Vertical (90°)	54.3	64.1	2.8	−0.148	141.3	−609.7	751

because it provides for large measurement areas, non-contact operation and high acquisition speed. The 3-D surface roughness parameters that were characterized in this study include arithmetic mean of the absolute of the ordinate values within a definition area (A) (S_a), root mean square value of the ordinate values within a definition area (A) (S_q), *Kurtosis* of the 3-D surface texture (S_{ku}), and the skewness of the 3-D surface texture (S_{sk}). The *Kurtosis* and skewness are statistical representations of the surface texture each determined by establishing a histogram of the heights of all measured points and the symmetry and presented by a deviation from an ideal Normal (i.e. bell curve) distribution [26]. The absolute height of the highest peak (S_p), the maximum valley depth (S_v) and the total height of the profile (S_z) were also used to characterize the surface roughness parameters of the EBM Ti-64 specimens. The mathematical evaluations of the surface parameters are shown below [29,30]:

$$S_a = \frac{1}{A}\int\int_A |Z(x,y)|\,dx\,dy \tag{1}$$

$$S_q = \frac{1}{A}\int\int_A (Z^2(x,y))\,dx\,dy \tag{2}$$

$$S_{ku} = \frac{1}{S_q^4}\int\int_A (Z^4(x,y))\,dx\,dy \tag{3}$$

$$S_{sk} = \frac{1}{S_q^3}\int\int_A (Z^3(x,y))\,dx\,dy \tag{4}$$

Surface characteristics and morphology were also studied via SEM using the Inspect-F50 (FEI, Oregon, USA) SEM operated with an accelerating voltage of 20 kV.

Results

Surface characterization

Table 1 shows the results of the surface characteristics of the EBM discs characterized through white light interferometry. The topographic 3-D views of the horizontal (0°), inclined (55°) and vertical (90°) EBM Ti-64 surface are shown with their corresponding S_a values in Fig. 2. The scanning electron microscope images in Fig. 3 show the surface topography morphologies of the three representative EBM Ti-64 parts at two different magnifications. It can be seen that different topographies on the Ti-64 discs were achieved as a result of the anisotropic character of the layer by layer generation process [31]. It can be deduced from Table 1, Fig. 2, Fig. 3 that the electron beam melted specimens have a relatively rough surface in terms of the S_a due to the various processing parameters including the starting powder particle size and the layer thickness selected as a consequence. Although the part orientation in AM has been reported to be the dominant parameter affecting the surface quality, reducing the layer thickness has also been reported to reduce the so-called staircase effect thereby improving the surface quality [8]. However in this study the layer thickness was selected according to Arcam AB's recommendations.

Table 1 also confirms that the least rough surface was obtained on the horizontal (0°) orientation of the Ti-64 within EBM chamber (S_a and S_q). This is attributed to the ability of the EBM machine to melt all the powder when the powder is exposed to the beam source at angles close to the normal direction. On the EBM system, the actual melting and welding together of powder particles takes place on the horizontal (0°) plane. The EBM horizontal (0°) sample also had a smallest value of the maximum valley depth (depth of the lowest point (S_v)) also due to the complete melting of powder particles. This depth feature is due to the presence of lines which occur as a result of melt tracks based on the beam hatching strategy. The beam hatching path yielded a pattern of parallel troughs 200 μm wide as can be seen in Figs. 2(a) and 3 (horizontal (0°)).

The inclined (55°) and vertical (90°) EBM surfaces are shown to have rough surfaces and this is attributed to adherent unmelted powder particles and the layering or staircase effect [32]. The topographic 3-D views in Fig. 2 (b and c) and the SEM micrographs

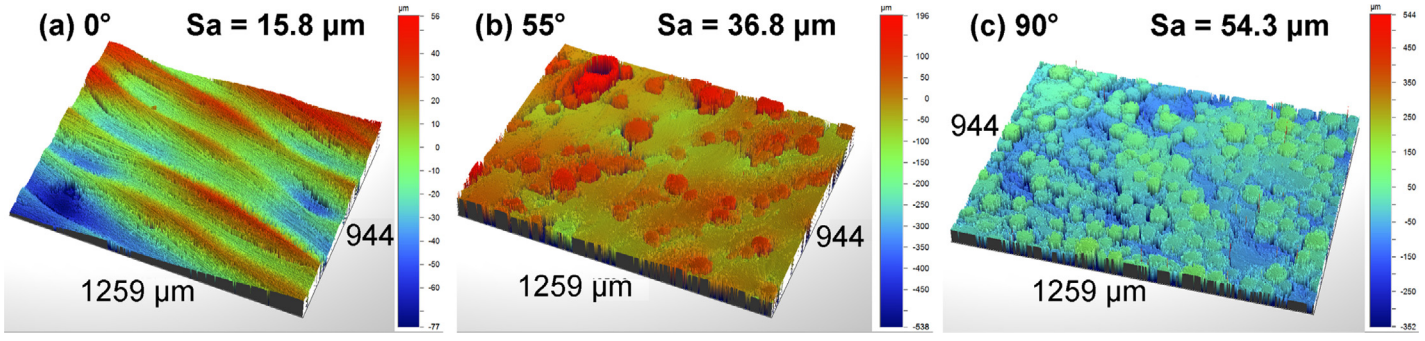

FIGURE 2

Topographic 3-D view of EBM Ti-64 horizontal (0°), inclined (55°) and vertical (90°) surfaces showing corresponding S_a values.

Please cite this article in press as: A.T. Sidambe, Met. Powder Rep. (2017), http://dx.doi.org/10.1016/j.mprp.2017.02.003

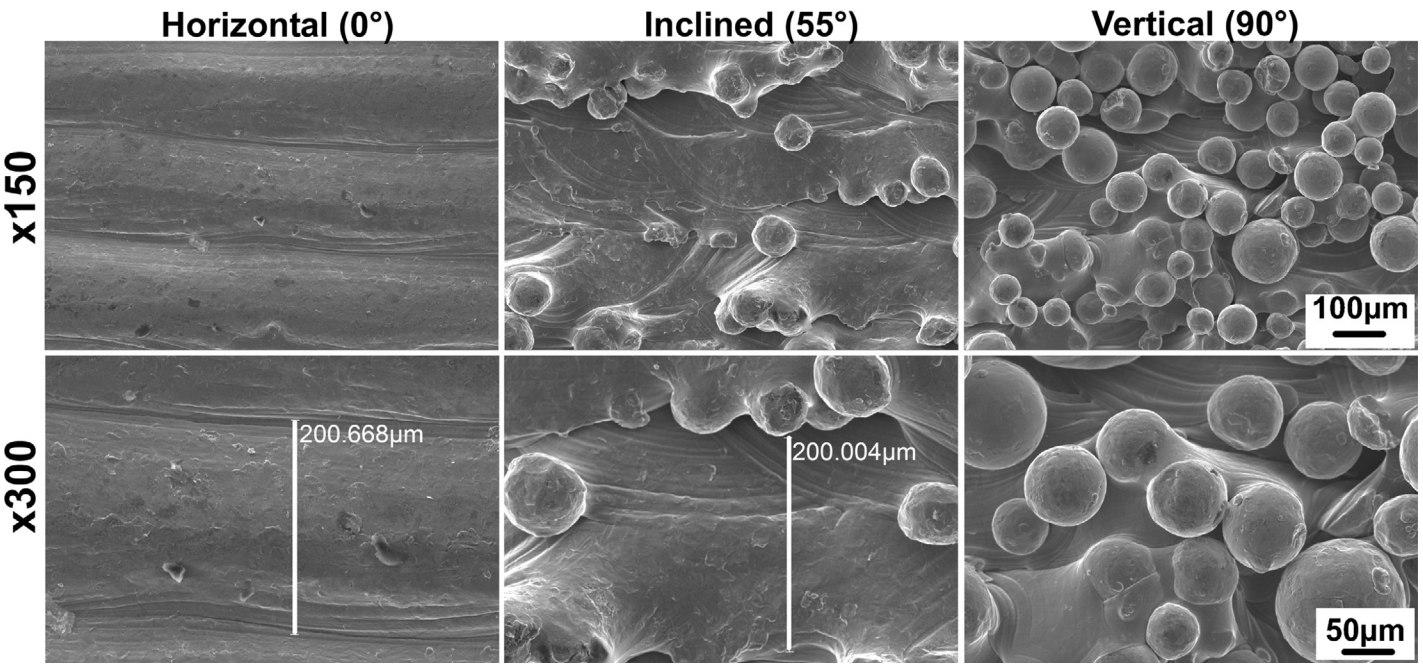

FIGURE 3

SEM surface topography comparing the horizontal (0°), inclined (55°) and vertical (90°) EBM Ti-64 components. The bottom row shows the micrographs at higher magnifications.

in Fig. 3 confirm the presence of adherent unmelted powder particles. The inclination of samples in the build chamber resulted in a combination of regions of smooth completely melted powder and regions of rough morphology due to unmelted powder particles, leading to a less rough 3-D surface profile (S_a and S_q) of the inclined (55°) orientation than of the vertical (90°) where the unmelted powder particles were more densely populated. The highest peak value (S_p) was obtained from the specimens in the inclined (55°) orientation whereas the highest valley depth value (S_v) was obtained from vertical (90°) EBM samples. It can be seen from Table 1 that S_p and S_v were considerably higher in the inclined (55°) and vertical (90°) samples than on the horizontal (0°) EBM. Overall, the vertical distance from deepest valley to highest peak within the measured area (S_z) was obtained on the inclined (55°) oriented EBM sample indicating considerable displacement of the unmelted adherent powder particles.

The 3-D surface texture analysis used in this study has the advantage of that the amplitudes mentioned above can be more accurately interpreted in terms of distribution and functionality of parameters. The surfaces have been characterized through the use of parameters which employ statistical techniques (S_{sk} and S_{ku}) and they have provided attributes of the surface such as amplitude variation [33]. Thus the *Kurtosis* of the 3-D surface texture S_{ku} that was measured and calculated from the horizontal (0°) and vertical (90°) surface was found to be less than the norminal value of 3 (i.e. $S_{ku} < 3$). This result shows that the form of the surface roughness height distribution on these surfaces was found to be squashed (dull peaks) with larger edge radius [26]. The *Kurtosis* is a yardstick for determining the sharpness of a surface and in the results obtained here, the surface texture can be interpreted as the less likely to initiate part failure. Furthermore the values of the *Kurtosis* obtained for the horizontal (0°) and the vertical (90°) are close to 3, indicating less randomness of the surface heights. On the inclined (55°) EBM sample, the S_{ku} was of a value greater than 3 (i.e. $S_{ku} > 3$) which means the surface has relatively small edge radius and the accumulation of powder particles on edges lead to peaks acquiring sharp profiles. The inclined surface of the EBM Ti-64 is therefore more susceptible to stress gathering regions and this exacerbated by the fact that a value of 6.1 was obtained for the Kurtosis, indicating increasing randomness of the surface heights. From these areal surface texture profiles resultant from part orientation, it becomes clear why considerations for design and part placement are important for the EBM of Ti-64.

The skewness of the 3-D surface texture S_{sk} that was measured and calculated from the inclined (55°) surface was found to have a positive value (i.e. $S_{sk} > 0$) which implies that the degree of skew (the symmetry of peaks and valleys about the average surface at the center) is downward relative to the average line. Therefore the surface was found to be predominated by peaks [34]. On the horizontal (0°) and vertical (90°) surfaces, the S_{sk} value was negative (i.e. $S_{sk} < 0$) and therefore the degree of skew is upward relative to the average line, indicating surfaces predominated by valleys [34]. However the values of the skewness were close to zero on the horizontal (0°) and vertical (90°) surfaces, indicating that the predominance of the valleys was not by a significantly high margin (i.e. the surface profile was close to comprising of equal valleys and peaks).

Discussion

The surface quality of Ti-64 components fabricated using the EBM process depends on a number of processing parameters but in this study the beam current, offset focus, scan speed, layer thickness and powder particle size distribution were kept constant, with the only variable being part orientation in the build chamber. The results revealed that different surface topographies can be obtained as a result of orientation in the EBM build chamber

Please cite this article in press as: A.T. Sidambe, Met. Powder Rep. (2017), http://dx.doi.org/10.1016/j.mprp.2017.02.003

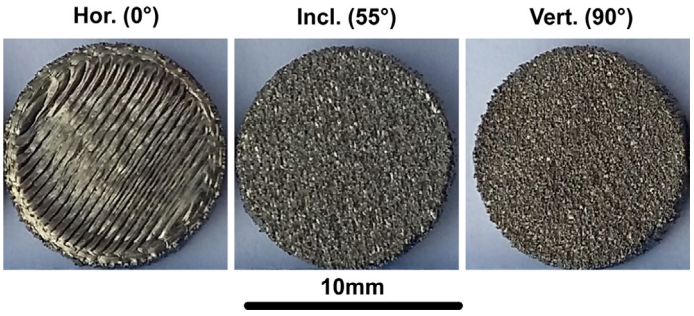

FIGURE 4

Photograph showing the manufactured Ti-64 discs and the resultant different surface finishes.

and that the surface roughnesses of the Ti-64 discs were in the micrometre scale range. It has also been possible to demonstrate that the topography of AM surfaces are suitably represented by 3-D areal surface parameters and that with these 3-D parameters it is possible to carry measurements of a higher statistical significance.

Figure 4 is a series of photographs showing the manufactured Ti-64 discs and the three different surface roughnesses that were obtained by orienting the builds in horizontal (0°), inclined (55°) and vertical (90°) orientations in the EBM build chamber. The photographs confirm that horizontal (0°) surface has a smoother surface texture with some lines present whereas the inclined (55°) and vertical (90°) surfaces appear rougher. However, it is more difficult to distinguish between the inclined and vertical surfaces using the naked eye and in addition, the similarities between the horizontal and the vertical surface roughness composition could be established mathematically using Eqs. (3) and (4).

The roughness values outlined in Table 1, the topographic 3-D views in Fig. 2 and the SEM micrographs in Fig. 3 indicate that there is a larger volume of more densely populated partial melted adherent particles as a direct result of minimum of exposure to the electron beam of the vertical (90°) orientation. The inclined (55°) orientation results suggest that the volume of partially melted particles is reduced because beam energy per unit volume (stepwise melting) is increased in comparison to the vertical (90°) surface. The horizontal (0°) surface had no unmelted powder particles because that is where beam energy is maximized, but there are lines and grove valleys (troughs) as a result of melt tracks. Based on these melting mechanisms, the analysis concerning a correlation between the part orientation angle and the average roughness (S_a) as well as the root mean square average roughness (S_q) is therefore expected to confirm the relationship between

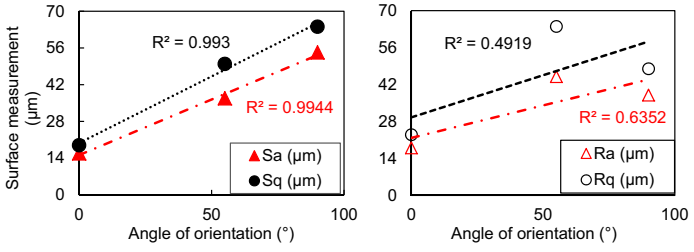

FIGURE 5

Correlation of S_a and S_q with the angle of orientation in comparisons with the correlation of R_a and R_q measured on the same surface.

these two ordinate values with the angle of part orientation according to established AM surface roughness models of similar parameters of R_a and R_q [35–37]. Furthermore our study is expected to form a linear relationship because the relatively larger layer size used. Figure 5 shows that the correlation coefficients for S_a and S_q were 0.9944 and 0.993 respectively as the surface roughness ordinate values increased with the angle of orientation and this is considered to be excellent correlation. For the 2-D values of R_a and R_q the correlation coefficients were 0.6352 and 0.4914 respectively and this is considered to be poor correlation.

The fact that a significantly high measure of roughness was detected on a surface where the powder is completely melted renders it imperative to distinguish between the surface features (i.e. troughs) on the horizontal (0°) surface and those detected in the other two surfaces (55° and 90°). Troughs are clearly elongated in one direction whilst the features in the other samples could be classified as pits. Furthermore, in order to demonstrate the advantage of 3-D analysis, it has been shown that this analysis can detect troughs whilst 2-D has limitations [33], it essential to discuss the surface topographies in terms of the width, height and depth of the features.

Thus, the horizontal (0°) and vertical (90°) surfaces have been reported in the Results section to have squashed texture (dull peaks with large edge radius) predominated by valleys whereas the inclined (55°) EBM sample had relatively small edge radius, predominated by peaks. It is apparent therefore that the texture of the inclined surface differs from the other two surfaces (horizontal and vertical). In additive manufacturing the smaller powder particles contribute towards surface roughness through an effect known as balling [38]. This arises as a result of a broken melt pool due to a large thermal variation between the center of the melt pool and its edges. Therefore the melt pool becomes unstable and breaks off into small entities to reduce its inner tensions [8].

Conclusion

In this study Ti-64 discs with different surface topographies were successfully built using the advanced EBM technique. This study has demonstrated that electron beam melting can be used to fabricate components with specific surface roughnesses. This study has shown that there may be complexities associated with EBM parts due to part orientation in build chamber. The results showed that when fabricating parts in the EBM, there is a trade-off between factors like orienting in the horizontal (0°) where in most cases the build height is reduced but there may be a requirement for support systems. Whereas inclining the component may lead to rougher surface finish and increased build height when avoiding the need for support system during processing. The selection of the surface parameters has addressed the inadequacies of two-dimensional (2-D) surface analysis through the analysis of 3-D surface topography data and surface morphology characterization. Through the selected white light interferometry system, it has been possible to measure an adequate surface area to achieve a reliable analysis of Ti-64 EBM surface. Finally, it would also be worth investigating whether surface parameter variations due to the nature of the Ti-64 EBM surface features do occur. Further studies should be carried out to investigate whether the inherent characteristics of Ti-64 EBM surfaces play an important role in the parameter variation rather than the measuring and data [27,33].

Please cite this article in press as: A.T. Sidambe, Met. Powder Rep. (2017), http://dx.doi.org/10.1016/j.mprp.2017.02.003

Acknowledgements

The author sincerely thanks Professor Iain Todd from the Materials Science and Engineering Department and Professor Paul Hatton from the School of Clinical Dentistry at the University of Sheffield for their assistance. Many thanks also go to Dr. Fatos Derguti and the staff at the Mercury Centre (University of Sheffield) for help with fabrication of the EBM Ti-64 discs. Finally, the author would like to thank the Wellcome Trust for providing financial support through the Institutional Strategic Support Fund (ISSF) at the University of Sheffield to conduct this research.

References

[1] A. Safdar, H.Z. He, L.Y. Wei, A. Snis, L.E.C. de Paz, Rapid Prototyping J. 18 (2012) 401–408. , http://dx.doi.org/10.1108/13552541211250391.
[2] P. Fox, S. Pogson, C.J. Sutcliffe, E. Jones, Surf Coat. Tech. 202 (2008) 5001–5007.
[3] A.T. Sidambe, I.A. Figueroa, H.G.C. Hamilton, I. Todd, J. Mater. Process. Tech. 212 (2012) 1591–1597. , http://dx.doi.org/10.1016/j.jmatprotec.2012.03.001.
[4] F.H. Froes, Adv. Mater. Process. 170 (2012) 16–22.
[5] A. Sidambe, I. Todd, P. Hatton, Mater. Sci. Forum (2015) 145–151, 10.4028/www.scientific.net/MSF.828-829.145.
[6] A.T. Sidambe, Materials 7 (2014) 8168–8188. , http://dx.doi.org/10.3390/ma7128168.
[7] F.H. Froes, Adv. Mater. Process. 170 (2012) 26–29.
[8] Tobias Grimm, Georg Wiora, W. Gerd, Surf. Topogr.: Metrol. Properties 3 (2015) 014001.
[9] R. van Noort, Dent. Mater. 28 (2012) 3–12. , http://dx.doi.org/10.1016/j.dental.2011.10.014.
[10] D.A. Hollander, T. Wirtz, M. von Walter, R. Linker, A. Schultheis, O. Paar, Eur. J. Trauma 29 (2003) 228–234. , http://dx.doi.org/10.1007/s00068-003-1332-2.
[11] O. Ivanova, C. Williams, T. Campbell, Rapid Prototyping J. 19 (2013) 353–364. , http://dx.doi.org/10.1108/Rpj-12-2011-0127.
[12] G. Chahine, M. Koike, T. Okabe, P. Smith, R. Kovacevic, JOM 60 (2008) 50–55. , http://dx.doi.org/10.1007/s11837-008-0148-2.
[13] S.S. Al-Bermani, M.L. Blackmore, W. Zhang, I. Todd, Metall. Mater. Trans. A 41A (2010) 3422–3434. , http://dx.doi.org/10.1007/s11661-010-0397-x.
[14] A.T. Sidambe, I. Todd, P.V. Hatton, Powder Metall. 59 (2016) 57–65. , http://dx.doi.org/10.1080/00325899.2016.1153278.
[15] J. Lv, Z. Jia, J. Li, Y. Wang, J. Yang, P. Xiu, K. Zhang, H. Cai, Z. Liu, Adv. Eng. Mater 17 (2015) 1391–1398. , http://dx.doi.org/10.1002/adem.201400508.
[16] L.E. Murr, K.N. Amato, S.J. Li, Y.X. Tian, X.Y. Cheng, S.M. Gaytan, E. Martinez, P.W. Shindo, F. Medina, R.B. Wicker, J. Mech. Behav. Biomed. 4 (2011) 1396–1411. , http://dx.doi.org/10.1016/j.jmbbm.2011.05.010.
[17] E. Hernández-Nava, C.J. Smith, F. Derguti, S. Tammas-Williams, F. Leonard, P.J. Withers, I. Todd, R. Goodall, Acta Mater. 108 (2016) 279–292. , http://dx.doi.org/10.1016/j.actamat.2016.02.029.
[18] T. Grimm, G. Wiora, G. Witt, Surf. Topogr.: Metrol. Properties 3 (2015) 014001.
[19] A.T. Beaucamp, Y. Namba, P. Charlton, S. Jain, A.A. Graziano, Surf. Topogr-Metrol. 3 (2015) 024001, http://dx.doi.org/10.1088/2051-672x/3/2/024001.
[20] R.K. Leach, Characterisation of Areal Surface Texture, Springer, 2013.
[21] A.T. Sidambe, I. Todd, P. Hatton, Proc. Euro PM 2015 Congress & Exhibition, 2015.
[22] V.R. Kearns, R.J. McMurray, M.J. Dalby, in: R. Williams (Ed.), Surface Modification of Biomaterials, Woodhead Publishing, 2011, pp. 169–201.
[23] G. Stevenson, S. Rehman, E. Draper, E. Hernandez-Nava, J. Hunt, J.W. Haycock, Biotechnol. Bioeng. (2015), http://dx.doi.org/10.1002/bit.25919.
[24] C.J. Smith, M. Gilbert, I. Todd, F. Derguti, Struct. Multidisciplinary Optimization (2016) 1–17.
[25] N. Shen, K. Chou, ASME 2012 International Manufacturing Science and Engineering Conference collocated with the 40th North American Manufacturing Research Conference and in participation with the International Conference on Tribology Materials and Processing, American Society of Mechanical Engineers, 2012, pp. 287–295.
[26] J. Kundrak, K. Gyani, V. Bana, Int. J. Adv. Manuf. Tech. 38 (2008) 110–119. , http://dx.doi.org/10.1007/s00170-007-1086-9.
[27] P. Stavroulakis, R. Leach, Rev. Sci. Instrum. 87 (2016) 041101.
[28] A. Triantaphyllou, C.L. Giusca, G.D. Macaulay, F. Roerig, M. Hoebel, R.K. Leach, B. Tomita, K.A. Milne, Surf. Topogr. Metrol. Properties 3 (2015) 024002.
[29] BS EN ISO 25178-2:2012. Geometrical product specifications (gps)-surface texture: Areal (part 2: Terms, definitions and surface texture parameters).
[30] BS EN ISO 25178-1:2016. Geometrical product specifications (gps)-surface texture: Areal (part 1 - indication of surface texture).
[31] S. Ponader, E. Vairaktaris, P. Heinl, C.v. Wilmowsky, A. Rottmair, C. Körner, R.F. Singer, S. Holst, K.A. Schlegel, F.W. Neukam, et al. J. Biomed. Mater. Res. Part A 84A (2008) 1111–1119. , http://dx.doi.org/10.1002/jbm.a.31540.
[32] G. Pyka, G. Kerckhofs, I. Papantoniou, M. Speirs, J. Schrooten, M. Wevers, Materials 6 (2013) 4737–4757.
[33] W.P. Dong, P.J. Sullivan, K.J. Stout, Wear 159 (1992) 161–171. , http://dx.doi.org/10.1016/0043-1648(92)90299-N.
[34] M. Lombardo, S. Talu, M. Talu, S. Serrao, P. Ducoli, J. Cataract Refract. Surg. 36 (2010) 1573–1578. , http://dx.doi.org/10.1016/j.jcrs.2010.06.031.
[35] G. Strano, L. Hao, R.M. Everson, K.E. Evans, J. Mater. Process. Tech. 213 (2013) 589–597. , http://dx.doi.org/10.1016/j.jmatprotec.2012.11.011.
[36] D. Ahn, H. Kim, S. Lee, J. Mater. Process. Tech. 209 (2009) 664–671. , http://dx.doi.org/10.1016/j.jmatprotec.2008.02.050.
[37] C.J. Luis Pérez, J. Vivancos Calvet, M.A. Sebastián Pérez, J. Mater. Process. Tech. 119 (2001) 52–57. , http://dx.doi.org/10.1016/S0924-0136(01)00897-4.
[38] K. Mumtaz, N. Hopkinson, Rapid Prototyping J. 15 (2009) 96–103. , http://dx.doi.org/10.1108/13552540910943397.

Please cite this article in press as: A.T. Sidambe, Met. Powder Rep. (2017), http://dx.doi.org/10.1016/j.mprp.2017.02.003